

# Isostatic compensation in the Western-Central Betic Cordillera (South Spain) caused by erosional unloading from the Messinian to the present: the emergence of an orogen

*Compensación isostática en la Cordillera Bética Occidental (Sur de España) causada por descarga erosiva desde el Messiniense hasta la actualidad: la emersión de un orógeno*

Javier Elez<sup>1</sup>, Pablo G. Silva<sup>2</sup>, Pedro Huerta<sup>2</sup> and Antonio Martínez-Graña<sup>1</sup>

<sup>1</sup> Depto Geología, Universidad de Salamanca, Facultad de Ciencias, Plaza de la Merced s/n, 37008 Salamanca. j.elez@usal.es; amgranna@usal.es.

<sup>2</sup> Depto Geología, Universidad de Salamanca, Escuela Politécnica Superior de Ávila, Avda. Hornos Caleros 50, 05003 Ávila. pgsilva@usal.es; phuerta@usal.es.

## ABSTRACT

In the Western-Central Betic Cordillera (WCBC), the Messinian Salinity Crisis triggered and important fluvial denudation, removing millions cubic meters of rocks from the Mediterranean slope of the emergent orogen. We offer an evaluation of the subsequent isostatic response calculating in a GIS environment the geophysical relief ( $g_r$ ) values (denudation plate and continuous models) and also surface uplift (Airy isostasy) for 48 drainage basins (spatial isostatic units). Higher  $g_r$  (major denudation) values are obtained consistently at the Mediterranean side of the ancient water divide (328-465 m) and noticeable lower (<235 m) in the Atlantic slope. The obtained  $g_r$  models show a similar asymmetric distribution. Comparison with published uplift models based on stratigraphic markers and landforms in the zone confirms that near the 45-50% of the total uplift of the WCBC was triggered during the MSC. Calculated surface uplift for the Mediterranean ( $291 \pm 20$  m) and Atlantic ( $179 \pm 20$  m) slopes indicate uplift rates during the MSC of 0.18 mm/yr in the Mediterranean (practically null in the Atlantic). Consequently, isostatic uplift caused by fluvial erosional unloading can be identified as one of the main processes controlling the landscape evolution in the zone during and after the MSC

**Key-words:** geophysical relief, isostatic rebound, denudation, MSC, landscape modification.

Geogaceta, 64 (2018), 103-106  
ISSN (versión impresa): 0213-683X  
ISSN (Internet): 2173-6545

## Introduction

The Western-Central Betic Cordillera (WCBC; Fig. 1) suffered a complex paleogeographic evolution during late Neogene times (e.g., Guerra-Merchán *et al.*, 2010). This evolution is closely related to the latest stages of development of the Gibraltar arc (e.g., Mattei *et al.*, 2006) and involves (among other processes) the closure and desiccation of the Mediterranean basin du-

ring the Messinian Salinity crisis (MSC; Hsü *et al.*, 1977) and the later catastrophic Zanclean flooding of the Mediterranean (Micallef *et al.*, 2018). In the central sector of the range (from Sierra de La Loja to the east, to El Torcal de Antequera and Serranía de Ronda) arcuate ridges elongated NE-SW are made up of Mesozoic Subbetic materials overthrust by the Flysch units (Fig. 1B). This ridge-line constituted the late Neogene water-divide between the Atlantic and Me-

## RESUMEN

En la Cordillera Bética Centro Occidental (CBCO), la MSC desencadenó una importante denudación fluvial, retirando millones de metros cúbicos de roca de la vertiente mediterránea del orógeno emergente. En este trabajo evaluamos la respuesta isostática subsiguiente calculando (en SIG) el relieve geofísico ( $r_g$ ) valores y modelos continuos de la placa de denudación) y la elevación superficial (isostasia de Airy) para 48 cuencas de drenaje (unidades isostáticas espaciales). Los valores más altos de  $r_g$  (mayor denudación) se han obtenido sistemáticamente en la antigua vertiente mediterránea (328-465 m), claramente menores en la vertiente Atlántica (<235 m). Los modelos continuos de  $r_g$  presentan la misma distribución asimétrica. La comparación con modelos de elevación publicados para la zona confirma que el 45-50% de la elevación total de la CBCO se produjo durante la MSC y las elevaciones isostáticas calculadas para la antigua vertiente mediterránea (c.  $291 \pm 20$  m) y Atlántica (c.  $179 \pm 20$  m) ofrecen tasas de elevación vertical de 0,18 mm/año durante la MSC en la mediterránea (y prácticamente cero en la atlántica). Por tanto, el rebote isostático producido por la denudación fluvial durante la MSC es uno de los procesos principales que controla la evolución vertical del relieve y el paisaje durante y después de la MSC.

**Palabras clave:** relieve geofísico, rebote isostático, denudación, CSM, modificación del relieve.

Recepción: 8 de febrero de 2018  
Revisión: 11 de abril de 2018  
Aceptación: 25 de abril de 2018

million cubic meters of rocks (Elez *et al.*, 2016). The isostatic response induced by the outsized erosional unloading caused by the MSC in the WCBC can be evaluated applying known methods (e.g., Menéndez *et al.*, 2008; Fernández-Ibáñez *et al.*, 2010). This paper presents the preliminary results of the isostatic study from the analysis of 48 individual drainage basins within the WCBC (Fig. 1A) in a GIS environment. In addition, comparison with the results obtained from Elez *et al.* (2016) regarding vertical uplift distribution from the Messinian to Recent in the Guadalorce fluvial basin allows the development of innovative paleotopographic and paleogeodetic scenarios for the entire WCBC.

## Methodology

The geophysical relief ( $g_r$ ) is defined as the result in meters from dividing the total eroded volume by the total area of a single drainage basin ( $g_r = m^3/m^2$ ) and is equivalent to the thickness (in meters) of the theoretical plate of denudated material by fluvial erosion (Small and Andersson, 1998). Consequently, the first step is to delimit the drainage divides (and calculate the basin area) in order to model the pre-incision surface and calculate the total eroded volume. This workflow has been applied to 48 basins in the WCBC (Fig. 1A), discarding the smallest ones ( $<15 \text{ km}^2$ ). The study area is limited by the Guadalquivir basin to the North and the Sierra Nevada range to the East. A 40m/pixel DEM of the study area (*Centro Nacional de Información Geográfica, CNIG-IGN*) was used all along the modelling process.

From the ridgelines delimiting the individual drainage basins and to obtain a continuous raster-model of the pre-incision surface (i.e., "ridgeline surface"), we proceed to extract the nodes of the polylines defining the present ridgelines and transformed them to point features. The elevation of these point features come from the topographic DEM, and the calculation of a first model of the "ridgeline surface" is obtained using a tense spline interpolation, which offered the best results. The "ridgeline surface" must envelop, form fitting, the whole drainage basin and all its internal reliefs (e.g., Fig. 2), since it is intended to set the relative uniform slope-topography before fluvial incision. The obtained models should overlie all internal reliefs within in-

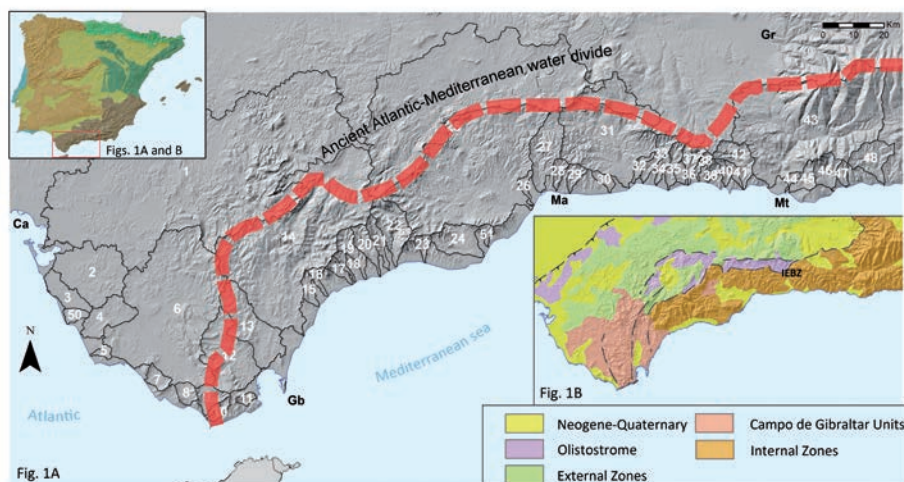


**Fig. 1. A)** Location of the studied fluvial basin (numbered) within the Western-Central Betic Cordillera, includes de approximated location of the Messinian Atlantic-Mediterranean water divide, dashed line, **B)** Geology of the area displaying the more relevant geological units. Ca: Cádiz, Gb: Gibraltar, Gr: Granada, Ma: Málaga, Mt: Motril. See color figure in the web.

*Fig. 1. A)* Localización de las diversas cuencas fluviales estudiadas (numeradas) dentro de la Cordillera Bética Occidental (CBCO), incluyendo la localización aproximada de la antigua divisoria de aguas entre el Atlántico y el Mediterráneo durante el Messiniense (línea discontinua), *B)* Esquema geológico de la zona estudiada en la que se muestran las unidades geológicas más relevantes. Ca: Cádiz, Gb: Gibraltar, Gr: Granada, Ma: Málaga, Mt: Motril. Ver figura en color en la web.

dividual basins, but typically some reliefs arise above the calculated "ridgeline surface" mainly in basins with complex morphology, geological evolution, recent volcanism and/or tectonics (e.g., Menéndez *et al.*, 2008). In these cases, more elevation points must be added at these protruding areas to guide the modelling processes and to ensure that the final ridgeline surface model completely overlies all internal reliefs. Typically this can take few iteration steps. This method assumes that the ridges have not been eroded, and hence the computed results are conservative. The GIS-based analysis offers two results (see Figs. 2 and 3). 1) The overall  $g_r$  value for each drainage basin from the computation of the total volume between the "ridgeline surface" and the present topography divided by the 2D area of the basin (Fig. 3C). 2) A  $g_r$  model from the subtraction of the "ridgeline surface" minus the present topographic DEM. The  $g_r$  model represents the continuous distribution of the geophysical relief (denudated rock-mass) in meters for spatial units of pixel size.

Surface uplift triggered by erosional unloading can be calculated applying elementary Airy-derived isostatic functions ( $\rho_c/\rho_m$ ), where  $\rho_c$  is the density of the crustal eroded material and  $\rho_m$  the density at the depth of compensation around the Moho. The use of standard values for  $\rho_c$  ( $2.67 \text{ g/cm}^3$ ) and  $\rho_m$  ( $3.33 \text{ g/cm}^3$ ) indicates

that the amount of uplift (i) per unit of denudation in meters is generally slightly less than the depth of fluvial dissection per unit area (Gilchrist *et al.*, 1994).

## Geophysical relief models for the Western-Central Betic Cordillera

The  $g_r$  model of the Guadalorce basin (the more complex basin) evidence that major denudation (higher  $g_r$  values) is concentrated in the southern half of the basin (Fig. 2C), coinciding with its ancient Mediterranean slope exposed to the relevant sea-level fall occurred during the MSC (e.g. Fleckert *et al.*, 2015). Those higher  $g_r$  values appear as NW-SE linear features in the  $g_r$  model (Fig. 2C). The computed values at these zones reach maximum of ca. 900 m (concentrated in the gorges zone), but mean  $g_r$  values of ca. 400 - 500 m are widely extended in the southern half of the basin. On the contrary, the northern portion of the basin has lower mean  $g_r$  values of ca. 250 m. This asymmetry in fluvial dissection within the basin clearly evidences the younger fluvial capture of this northern half of the basin. The  $g_r$  mean value (denudation plate) for the Guadalorce basin is 348.57 m ( $1151.55 \text{ km}^3/3442.89 \text{ km}^2$ ). However denudation is asymmetrically distributed within the basin between its old Atlantic (northern sector) and Mediterranean (southern sector) slopes. In the nor-

thern sector the denudation plate is of 281.16 m (538.51 km<sup>3</sup>/ 1972.70 km<sup>2</sup>), whilst in the south is of 442.06 m (611.99 km<sup>3</sup>/ 1465.95 km<sup>2</sup>). This asymmetry in the denudation values indicate that about 61% of fluvial erosion concentrated in the old Mediterranean slope of the basin.

In the Guadalhorce basin this differential erosional unloading occurs mainly during the MSC (Elez *et al.*, 2016). Later, Pliocene to Quaternary fluvial incision reshaped the late Neogene landscape in the old Mediterranean slope generating impressive gorges and the eventual capture of the old Atlantic slope of the basin (Elez *et al.*, 2016).

A comparable N-S asymmetric distribution of  $g_p$  values also occurs in the Vélez river basin (N° 31 in Fig. 1A) and other minor basins, likewise crossed by the ancient Atlantic-Mediterranean water divide. In this case, values for the denudation plates are of 186.89 m in the northern sector and 407.55 m in the southern one. The value of the denudation plate for the entire basin is of 357.95 m, similar to that computed for the Guadalhorce basin.

Figure 3 illustrates the spatial distribution of the computed  $g_p$  values for the whole WCBC from the overall "ridgeline surface" model (Fig. 3A). The regional picture clearly shows a different distribution of  $g_p$  values at both sides of the ancient water-divide (Fig. 3B), with wide areas exceeding values of 500 m and maximum values of about 1200-1500 m in the ancient Mediterranean slope while values near 100-400 dominate in the Atlantic side. Figure 3C illustrates the denudation plates for each analyzed basin. The basins located at the ancient Mediterranean slope display quite significantly greater  $g_p$  values (328 - 465 m for the largest basins) than those located at the Atlantic slope (< 235 m). This asymmetric distribution is noticeable even in the case of the smaller basins and evidences (and is interpreted here as) the influence of the ancient late Neogene water divide in the differential denudation triggered by the MSC in the emergent orogeny.

### Isostatic uplift caused by erosional unloading: The example of the Guadalhorce basin

The computed surface uplift due to the erosional unloading ( $\rho_c/\rho_m=0.874$ ) is 233 ±20 m for the whole studied sector of the

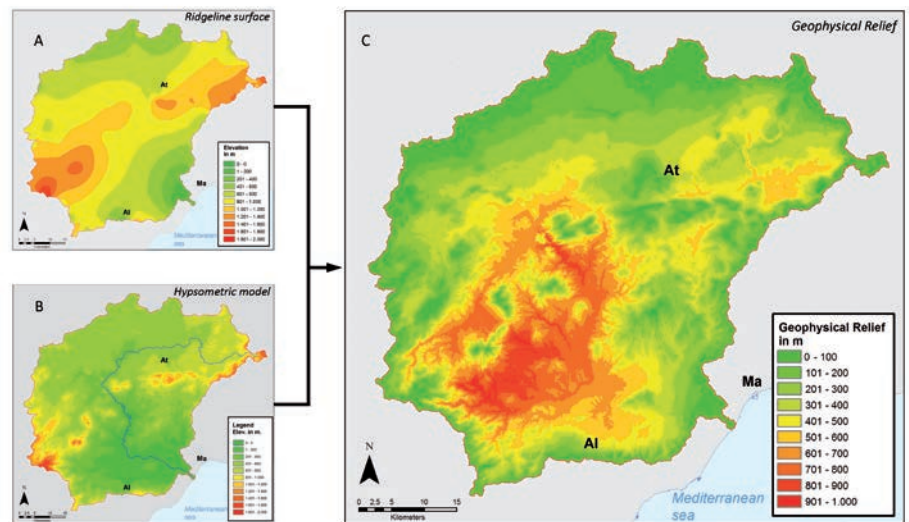


Fig. 2. Geophysical relief model of the Guadalhorce river basin. A) Ridgeline surface. B) Present hypsometric distribution. C) Geophysical relief model obtained from the subtraction of the previous models. Al: Alora, At: Antequera, Ma: Málaga. See color figure in the web.

Fig. 2. Modelo de relieve geofísico de la cuenca del río Guadalhorce. A) Modelo de Superficie de Divisoria. B) distribución hipsométrica actual. C) Modelo de Relieve Geofísico obtenido de la resta de los dos modelos previos. Al: Alora, At: Antequera, Ma: Málaga. Ver figura en color en la web.

Betics (WCBC) since the onset of the MSC. However, the values of uplift computed for the Mediterranean (c. 291 ±20 m) and Atlantic (c. 179 ±20 m) slopes are significantly different resembling the spatial distribution of  $g_p$  illustrated in figures 3B and C. A similar scenario occurs in the case of the Guadalhorce basin (Figs. 2 and 3). The computed uplift for the entire basin is of 304 ±20 m, but the values for its northern (245.79 ±20 m) and southern (386.44m ±20 m) sectors differ.

In the case of the Guadalhorce basin is possible to compare the  $g_p$  data with the paleotopographic and paleogeoid models developed by Elez *et al.* (2016), in detail, it is especially valuable the comparison with the late Messinian sea level surface (paleogeoid) deformation model (PDM). This is obtained from proxy elevation data of stratigraphic (late Tortonian to early Messinian littoral sediments in the zone presently located at elevations between 400 and 700 m Sanz de Galdeano and Alfaro, 2004) and geomorphologic nature uplifted about 650-700 m, (Elez *et al.*, 2016). These PDM models also show an approximation to the accumulated uplift from late Messinian to Recent (discounting the eustatic component). Although both kind of models ( $g_p$  and paleogeoid uplift) result from different conceptual approaches, the thickness of the denudation plate computed here ( $g_p = 348$  m) is similar to the uplift computed from paleogeoid models (345 m) since the

MSC obtained by Elez *et al.* (2016). Comparing the computed values of uplift obtained here (ca., 350 m) with the bulk uplift of the area coming from upraised late Neogene stratigraphic markers and landforms in the zone seems evident that near the 45-50% of the uplift was triggered by erosional unloading.

Since sea level is supposed to be uniform after the Zanclean refilling (e.g., Micallef *et al.*, 2018), the asymmetry in uplift values for the entire WCBC is a clear consequence of the stronger erosional rock removal caused by the sea-level fall during the MSC. Then, the difference of isostatic uplift between the Mediterranean (291 ±20 m) and Atlantic (179 ±20 m) slopes corresponds only to the uplift generated during the MSC, about 112 ±20 m, indicating uplift rates about 0.18 mm/yr in the Mediterranean slope and around null in the Atlantic one during the MSC.

### Conclusions

For the WCBC, a transect of more than 200 km along the Betic Cordillera, the spatial distribution of the geophysical relief (Figs. 3A and B) and subsequent isostatic uplift is strongly constrained by the ancient Messinian Atlantic-Mediterranean water divide (Fig. 1A), with the higher values to the ancient mediterranean slope. Results indicate that uplift triggered by erosional unloading can achieve near 45% of the total

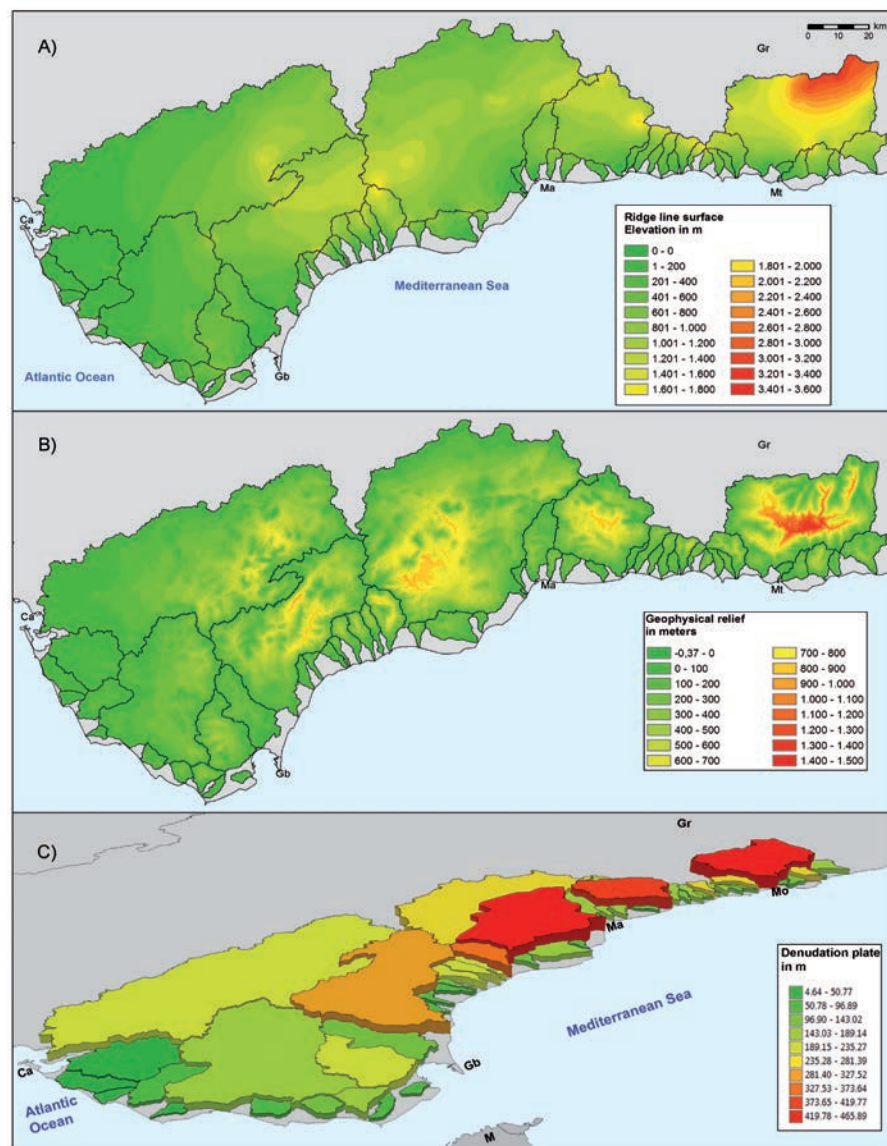


Fig. 3. Geophysical relief models of the WCBC. A) Ridge line surface. B) Geophysical relief model of the WCBC, showing a continuous distribution of the geophysical relief C) Bar map/diagram of the geophysical relief value (denudation plate) for each fluvial basin. In this case, the geophysical relief values for the basins of the Guadalhorce and Vélez rivers are divided following the ancient Atlantic-Mediterranean water divide, see justification in the text. Ca: Cádiz, Gb: Gibraltar, Gr: Granada, M: Morocco, Ma: Málaga, Mt: Motril. See color figure in the web.

Fig. 3. Modelos de relieve geofísico de la CBCO. A) modelo final de Superficie de Divisoria B) Modelo derelieve geofísico de la CBCO mostrando la distribución continua de los valores de Relieve Geofísico. C) Diagrama/mapa de barras representando los valores de relieve geofísico (placa de denudación) para cada una de las cuencas fluviales estudiadas. En este caso, los valores de relieve geofísico para las cuencas fluviales de los ríos Guadalhorce y Vélez se han dividido en dos siguiendo la traza de la antigua divisoria de aguas entre el Atlántico y el Mediterráneo, justificado en el texto. Ca: Cádiz, Gb: Gibraltar, Gr: Granada, M: Marruecos, Ma: Málaga, Mt: Motril. Ver figura en color en la web.

recorded uplift. Consequently, isostatic uplift caused by erosional unloading is identified as one of the main processes controlling the landscape evolution during and after the MSC in the WCBC.

### Acknowledgements

This study has been funded by the MI-NECO-FEDER Spanish research projects CGL2015-67169-P (QTETCSPAIN-USAL)

and 2009-2012 EUROCORES-TOPOMED PROGRAM through the Spanish research project CGL2008-03474-E/BTE (CSIC), produced by the USAL TopoMed-Spain Onshore Research Group. The authors are grateful for their comments to José Vicente Pérez Peña, Alejandro Jiménez Bonilla and Manuel Díaz Azpiroz, reviewers and editor of this work, which really improved the quality of the original manuscript and provide interesting ideas for future work.

### References

Elez, J., Silva, P.G., Huerta, P., Perucha, M.A., Civis, J., Roquero, E., Rodríguez-Pascua, M.A., Bardají, T., Giner Robles, J.L., and Martínez Graña, A. (2016). *Geomorphology* 275, 26-45.

Fernández-Ibañez, F., Pérez-Peña, J.V., Azor, A., Soto, J.I. and Azañon, J.M. (2010). *Geology* 38, 643-646.

Flecker, R., Krijgsman, W., Capella, W., de Castro Martins, C., Dmitrieva, E., Maysner, J.P., Marzocchi, A., Modestu, S., Ochoa, D., Simon, D., Tulbure, M., van den Berg, B., van der Schee, M., de Lange, G., Ellam, R., Govers, R., Gutjahr, M., Hilgen, F., Kouwenhoven, T., Lofi, J., Meijer, P., Sierro, F.J., Bachiri, N., Barhoun, N., Alami, A.C., Chacon, B., Flores, J.A., Gregory, J., Howard, Pancost, R., Vincent, S. and Yousfi, M.Z. (2015). *Earth-Science Reviews* 150, 365-392.

Gilchrist, A.R., Summerfield, M.A. and Cockburn, H.A.P. (1994). *Geology* 22, 963-966.

Guerra-Merchán, A., Serrano, F., Garcés, M., Gofas, S., Esu, D., Gliozzi, E. and Grossi, F. (2010). *Palaeogeography, Palaeoclimatology, Palaeoecology* 285, 264-276.

Hsü, K.J., Montadert, L., Bernoulli, D., Cita, M.B., Erickson, A., Garrison, R.E., Kidd, R.B., Mélières, F., Müller, C. and Wright, R. (1977). *Nature* 267, 399-403.

Martín, J.M., Puga-Bernabéu, A., Aguirre, J., Braga, J.C. (2014). *Revista de la Sociedad Geológica de España* 27, 175-186.

Mattei, M., Cifelli, F., Martín Rojas, I., Crespo Blanc, A., Comas, M., Faccenna, C. and Porreca, M (2006) *Earth and Planetary Science Letters* 250, 522-540.

Menendez, I., Silva, P.G., Martín-Betancor, M., Pérez-Torrado, F.J., Guillou, H. and Scaillet, S. (2008). *Geomorphology* 102, 189-203.

Micallef, A., Camerlenghi, A., Garcia-Castellanos, D, Cunarro Otero, D., Gutscher, M.A., Barreca, G., Spatola, D., Facchin, L., Geletti, R., Krastel, S., Gross, F., Urlaub, M. (2018). *Nature Scientific Reports* 8;1078, 1-8.

Sanz de Galdeano, C. and Alfaro, P. (2004). *Geomorphology* 63, 175-190.

Silva, P.G., Ribó, A., Martín-Betancour, M., Huerta, P., Perucha, M.A., Zazo, C., Goy, J.L., Dabrio, C.J. and Bardají, T. (2011). *In: Proceedings of the 2nd INQUA-IGCP-567*, 227-230.

Small, E.E. and Andersson, R.A. (1998). *Geology* 26, 123-136.